Study on Wind Loads Coefficients and Flow Field Characteristics Around the Parabolic Trough With Stiffeners

Dr.Mauwafak Ali.Tawfik
Mechanical Engineering Department, University of Technology /Baghdad
Dr.Bahaa.Ibrahim.Kazem
University of Baghdad
Haider.Hussein.Hamad
University of Baghdad
Email:Haider hussein2010@yahoo.com

Received on: 14/11/2011 & Accepted on:7/6/2012

ABSTRACT

In the current study, the numerical analysis of the flow field characteristics around the parabolic trough with stiffener of solar polar concentrating power system is performed. The presence of stiffener changes the velocity and pressure distribution around the trough and then the wind loads also changed. Wind loads (drag, lift and moment) coefficients for different wind speeds and angles of attack are simulated. Pressure distribution, velocity distribution and turbulent kinetic energy for different wind speeds and angles of attack are also simulated. To verify the numerical simulation, comparisons with experimental results are performed. Reproducing of experimental boundary condition is carried out in numerical simulations. The numerical simulations are performed by using computational fluid dynamics (CFD) package fluent 12.1. The results of this simulation show that the flow field characteristics are strongly related to angles of attack and trough orientation. Also the most important result of this study is that the presence of stiffener makes the trough a more bluff body than the trough without stiffener. This development of trough configuration will excite more vortexes shedding around the edges of trough.

Keywords: Parabolic trough with stiffener, CFD, wind loads, wind tunnel tests.

دراسة معاملات احمال الرياح وخصائص مجال الجريان حول الصحن ذو مقطع بشكل قطع مكافئ مع المصلدات

الخلاصة

تم في هذه الدراسة اجراء التحليل العددي لخصائص الجريان حول الصحن ذو مقطع بشكل قطع مكافئ والمستخدم في انظمة تركيز الطاقة الشمسية القطبي مع المصلدات. اثر وجود المسند على توزيع السرعة والضغط حول الصحن. تم ايجاد معاملات احمال الرياح عند سرع رياح مختلفة وزوايا هبوب مختلفة مع الصحن. كذلك تم ايجاد توزيع السرعة وتوزيع الضغط وتوزيع طاقة الاضطراب عند سرع رياح مختلفة وزوايا هبوب مختلفة مع الصحن. لغرض التاكد من صحة النتائج تمت مقارنة النتائج العددية مع نتائج عملية. التحليل العددي تم باستخدام برنامج ديناميك الموائع العددي

https://doi.org/10.30684/etj.30.18.13
2412-0758/University of Technology-Iraq, Baghdad, Iraq

(fluent12.1). اظهرت نتائج البحث ارتباط قوي بين قيم وتوزيع خصائص الجريان مع زوايا هبوب الرياح ووضع الصحن. كذلك فان من اهم نتائج الدراسة ان وجود المصلد جعل الصحن اكثر تعقيدا من الصحن بعدم وجود المصلد. اثر هذا التطوير في شكل الصحن على انبثاق الدوامات حول حافات الصحن.

INTRODUCTION

The solar thermal power (STP) plants are used to concentrate the heat on the working substance which used then in steam production process for electrical generation. Solar thermal power plants are primarily installed in flat terrain of high solar irradiation for achieving a high power density. The parabolic trough collector is considered to be the most suitable for concentration task. At flat terrain, the components of plants are subjected to severe aerodynamic problems. The parabolic trough is the main component which expose to such aerodynamic effects. The main environmental problems which affect the parabolic trough performance are the wind-induced vibration and trough instability to truck the sun accurately. To overcome these problems, comprehensive solutions should be investigated. The key of these solutions is the comprehensive study of flow characteristic around the parabolic trough and determine the effect of each parameter on the performance of the trough. These flow characteristics included the aerodynamic loads (drag, lift and moment), pressure distribution, turbulent kinetic energy and vortex field visualization. The estimation of all these parameter will give the base to introduce practical solutions for each aerodynamic problem. The dust accumulation on the interior surface of the parabolic trough is another problem can decrease the optical performance of the trough. The vibrational dust removal technique which used for cleaning the solar panels in aerospace vehicle can be the suitable solution to reduce the dust accumulation. This technique depends on the aerodynamic forces produced by wind and vibrational forces which can be induced by different techniques to moving the dust particles away from the surface of trough. The vortex induced vibration can be the suitable source for vibrational forces. The vortex shedding in the wake of the trough supplies fluctuating aerodynamic forces which will excite the structure to vibrate in specific frequency and amplitude. This approach requires a comprehensive study on the behavior of vortex shedding and the control on these forces to obtain the desired vibration used in dust removal technology. So, the most important point should be assigned here that the current investigation aims to study the flow field parameters around the parabolic trough to understanding the effect of these parameters on the dynamic response of the parabolic trough and make a suitable control on these parameters to reduces the undesired effects and at the same time to get a good benefit for vibrational dust removal technique. The study of flow field around any structure requires either experimental test performed in valid boundary layer wind tunnel or using computational fluid dynamics (CFD) package to solve the governing equations numerically and obtaining the desired results.

The studies of flow field and dynamic behavior of parabolic trough under the action of wind are very rare. L. M. murphy carried out a study to discuss the most

practical designs for the collector and the test procedures to evaluate the wind loading on the collector. The test results corresponding to numerous wind tests on heliostats, parabolic troughs, parabolic dishes, and field mounted photovoltaic arrays are discussed and the applicability of the findings across the various technologies is assessed [1]. J. A. Peterka et. Al. carried out a study to define mean and peak wind loads on parabolic dish solar collectors. Loads on isolated collectors and on collectors within a fie1d of collectors were obtained. A major intent of the study was to define wind load reduction factors for collectors within a field resulting from protection offered by upwind co1lectors, wind protective fences, or other blockage elements [2].

N. U. Gunasena performs a study to determine the feasibility of a novel solar collector design for large scale solar power generation. The design concept involved a large, fixed mirror dish in the shape of a spherical segment, with a tracking collector as opposed to a more traditional tracking concentrator with a fixed or tracking collector [3]. N. Hosoya and J.A. Peterka carried out comprehensive experimental study to determine the mean and maximum wind load coefficients on the parabolic trough in boundary layer wind tunnel. The wind loading on parabolic trough are determined for different angles of attack, for different wind speeds and for different turbulent intensity. This study showed that the wind loads coefficients are independent of the Reynolds number and turbulent intensity [4]. N. Naeeni, M. Yaghoubi are performed a two-dimensional numerical simulation of turbulent flow around a parabolic trough collector of the 250kW solar power plants taking into account the effects of variation of collector angle of attack, wind velocity and its distribution with respect to height from the ground. Various recirculation regions on the leeward and forward sides of the collector are observed, and both pressure field around the collector and total force on the collector are determined for each condition [5]. The current study aims to determine the flow field characteristics around the parabolic trough with stiffener. The flow characteristics include the mean wind loads coefficients (drag, lift and moment), pressure distribution, turbulent kinatic energy and vortex shedding visualization. The presence of stiffener will affect the flow field distribution around the trough. Numerical analysis is performed by using a suitable computational fluid dynamics (CFD) package fluent 12.1 to solve the governing equations and boundary conditions.

NUMERICAL RESULTS VERIFICATIONS

In order to verify the numerical results which are obtained from computational fluid dynamics package, the preliminary comparisons with experimental results should be performed. The experimental results which used in this verification are obtained from boundary layer wind tunnel tests performed in National renewable energy Laboratory [4]. These results included the wind loads coefficients on the parabolic trough in different azimuthal angles (pitch angles θ) and inclination (yaw angle ψ) and different values of Reynolds number. The validity of boundary-layer wind tunnel testing for wind loads on structures is based on similarity arguments and on model-to-full-scale test comparisons. The most important parameters which should be considered in similarity arguments are the mean wind velocity profile and the

turbulence intensity. The wind tunnel are designed to provide a modelled atmospheric boundary layer and a mean velocity power law exponent and turbulence structure in the modelled atmospheric boundary layer similar to that expected in open country. Numerical simulations have been performed to reproduce the experimental conditions in the wind tunnel. The model of the parabolic trough and angles of attack description which used in experimental tests is shown in figure (1) with scale 1/45. Also the mean wind velocity profile and turbulent intensity profile for experimental setup are shown in figure (2). The most important conclusion obtained from the experimental tests [4] that load coefficients of the solar collector were essentially independent of Reynolds number in a range realized in the wind tunnel, probably due to sufficiently high level of turbulence over the height of the collector modelled in a surface boundary layer flow. The effect of the turbulence was found to be insignificant as long as the turbulent approach flow was simulated properly in the wind tunnel. The comparisons between the experimental and numerical results are performed by using aerodynamics coefficients (drag and lift) for pitch angles (0˚, 30˚, 60˚, 90˚, 120˚, 150˚, 180˚), yaw angle equals to zero. Figures (3 &4) show these comparisons. These comparisons show that the numerical simulation has good agreement with experimental results for most azimuthal angles (pitch angle) except for some pitch angles. These discrepancies were appears because that the numerical simulation has some limitations in flow modelling around bluff bodies which expose severe aerodynamic conditions such as high pressure difference across the faces of tough and high vortex shedding near the edges of trough. Nevertheless the numerical results can be assumed to be a suitable approximation tool in evaluating the flow characteristics around the structures.

BOUNDARY CONDITIONS

In this study, numerical simulations have been performed to reproduce the experimental conditions in the boundary layer wind tunnel. The governing equations in atmospheric boundary layer are Reynolds Averaged Navier Stokes (RANS) equations and RNG-based k-ε turbulent scheme. The Reynolds-averaged Navier-Stokes (RANS) equations govern the transport of the averaged flow quantities, with the whole range of the scales of turbulence being modelled. The RANS-based modelling approach, therefore greatly reduces the required computational effort and resources, and is widely adopted for practical engineering applications[6]. The RANS equations are often used to compute time-dependent flows, whose unsteadiness may be externally imposed (e.g., time-dependent boundary conditions or sources) or self-sustained (e.g., vortex-shedding, flow instabilities) [6]. In (k- ε) models, the turbulent kinetic energy is k and viscous dissipation rate of turbulent kinetic energy is (ε). The RNG turbulence model is more responsive to the effects of rapid changes and streamlines curvature, flow separation, reattachment and recirculation than the standard k-ε model and it has been used widely for wind flow studies [7]. A power law boundary layer equation is used for the inlet boundary condition for the domain. The design wind speed is based on national wind load standard ASCE 7-98. The power-law exponent is obtained by a linear regression of wind data measured at different heights.

Figure (2) shows the mean wind velocity and turbulence intensity profiles simulated for the current study. As seen, the modelled boundary layer profiles compare well with those suggested by ASCE 7-98 for winds over an open country exposure (α=0.14) and the turbulent boundary layer with 21% turbulence intensity. At the edges of domain, the symmetry boundary will apply. Symmetry boundary conditions are used when the physical geometry of interest and the expected pattern of the flow solution have mirror symmetry. Also the Symmetry boundaries are used to reduce the extent of computational model to a symmetric subsection of the overall physical system [6]. The boundary condition at the trough surface is wall with free slip conditions. Wall boundary conditions are used to bound fluid and solid regions. At the outlet, pressure outlet boundary condition was applied. Pressure outlet boundary conditions require the specification of a static (gauge) pressure at the outlet boundary. For the current simulation the outlet pressure equal to zero.

NUMERICAL SIMULATION PROCEDURE

The numerical simulation of the current study is performed by using computational fluid dynamics package (fluent 12.1). The dimensions of the parabolic trough with stiffener which used in this numerical simulation are shown in figure (5). The parabolic part of the trough having equation $y=0.156(x^2/0.0625)$ where y and x in (m). The stiffener is arc of (75˚) and extended for (0.05m). The stiffener is made from the same material of trough. The presence of stiffener in this profile will make little changes to the trough from streamlined body to bluff body but at the same time, the structure will be more sophisticated. The domain of the current simulation is the boundary layer wind tunnel. The dimensions of the domain preliminary chosen to be the same of the experimental wind tunnel dimensions but it then modified to develop flow field independent of domain size and mesh density. Table (1) shows the domain size and mesh density corresponding to each pitch angle. The mesh density is also modified to ensure the numerical reliability of the obtained results. The results sensitivity to mesh density is performed by increasing the density and record the change in wind load coefficients (drag and lift) until the tolerance of sequence results become less than (10^{-5}). The table (2) shows the mesh density sensitivity analysis for typical case where the pitch angle is (60˚) and Reynolds number $2.7932*10^5$. The number and size of grid ere not constant along the domain and differ in number and size corresponding to pitch angles. The size of grid near the trough is very fine and gradually increases toward the edges of domain. Figure (6) shows the domain and the mesh density distribution through the domain. The numerical simulation is carried out for pitch angles (0˚, 30˚, 60˚, 90˚, -30˚, -60˚, and -90˚) and for Reynolds numbers ($2.7932*10^5$, $5.5866*10^5$, $8.3798*10^5$, and $11.173*10^5$). These Reynolds numbers are corresponding to inlet mean wind velocities (5, 10, 15, and 20) m/s. The figure (7) shows these pitch angles relative to wind stream direction. The flow field parameters which obtained from these simulations are wind loads coefficients (drag, lift and moment), pressure distributions around the parabolic trough corresponding to pitch angle, mean wind velocity distributions corresponding to each pitch angle and inlet mean wind velocity, turbulent

kinetic energy and vortex recirculation regions which are formed around the parabolic trough. The wind loads corresponding to each wind velocity are calculated simply by multiplying the wind loads coefficients which obtained from experimental or numerical simulations by the value of dynamic pressure corresponding to wind velocity and the leeward projected area of trough with respect to wind flow direction (appendix A). These forces are fluctuated in nature due to turbulent and the alternative vortex shedding. So, these forces will excite the structure to vibrate in specific frequency and magnitude depending on structure characteristics. This vibration can be controlled and used in dust removal techniques. All other parameters also can be used to determine the dynamic response of the trough to wind loading.

RESULTS AND DISCUSSIONS

Figures (8, 9, and 10) shows the results of wind loads coefficients (drag, lift and moment) corresponding to different pitch angles and yaw angle ($\psi = 0^{\circ}$). These results obtained from numerical simulation. Figure (8) shows the results of drag coefficient versus the pitch angles (-90°, -60°, -30°, 0°, 30°, 60°, and 90°). From this figure, it is obvious that the maximum value of drag coefficient at pitch angle (0°) which means that the trough aperture normal to wind flow direction while the minimum value at pitch angles ($+90^{\circ}$ and -90°) where the aperture of the trough is parallel to wind flow direction. Figure (9) shows the results of lift coefficient as a function of pitch angles.

From this figure, it is observed that the values of this coefficient fluctuated around the zero. Maximum positive value of lift coefficient occurs at pitch angle (-60°) and maximum negative value occurs at pitch angle ($+60^{\circ}$). Figure (10) shows the values of moment. These values are fluctuated around the zero. The moment coefficient values are small in comparison of drag and lift coefficient. The numerical simulation is repeated for wind speeds (5, 10, 15, and 20) m/s. The most important result is that the wind load coefficients are approximately constant at different Reynolds number. This result is also obtained from experimental tests which performed by [4]. In addition to wind loads, the flow characteristics are simulated such as velocity vector, pressure distribution and turbulent kinetic energy. Figure (11) shows the velocity vector at different velocities for pitch angle ($\theta=0^{\circ}$). Referring to this figure, it is observed that the pattern of velocity distribution around the trough didn't change with increasing the velocity except that the magnitude of velocity vector is changed. Figure (12) shows the pressure distribution around the parabolic trough for two velocities and pitch angle ($\theta = +60^{\circ}$). From this figure, it is clear that the pressure distribution around the trough is dependent of velocity. Also the pressure distribution around the trough is strongly dependent to pitch angle as illustrated in figure (13). Contours of velocity and pressure distribution around the trough show that many regions of vortex shedding are formed and this formation is strongly dependent on the trough orientation and wind direction. High vortex shedding regions are observed for pitch angle ($\theta = 0^{\circ}$) because that the trough at this pitch angle expose to severe aerodynamics conditions but these eddies formation decreases when the pitch angle increases until it reach to ($\theta = 90^{\circ}$). It is observed from figures of pressure distribution around the parabolic trough that the

maximum pressure zones are on the forward side of the collector while the minimum pressure zones are on the leeward side. The pressure difference between the forward and leeward is dependent on the orientation of the collector. The maximum difference occurs at pitch angle ($\theta = 0^{\circ}$) while the minimum pressure difference occurs at pitch angle ($\theta = \pm 90^{\circ}$) as illustrated in figure (14). The present configuration of the parabolic trough with stiffener makes the trough more bluff body than the trough without stiffener. This appears clearly from the figures of velocity and pressure distribution. The trough without stiffener has separation regions at the edges of the trough. This separation leads to high pressure difference at the edges especially at pitch angle close to zero. The presence of a curve stiffener increases the formation of recirculation zones because that the regions behind the stiffeners will be additional recirculation zones and this will lead to increase the fluctuating forces on the trough. So, the presence of stiffener is useful to improving the flow induced vibration concept which is useful for dust removal technology. Also, the distribution of turbulent kinetic energy is dependent on angle of attack. The maximum value of turbulent kinetic energy appears near the edges of trough for the angles of attack ($\theta = +30^{\circ}, +90$) as shown in figures (15) and (16) while the maximum value appears near the center of trough for angle of attack ($\theta = 0^{\circ}$) as shown in figure (17).

CONCLUSIONS

1-The wind load coefficients are very dependent of angle of attack (pitch angle)
2-The wind load coefficient are independent of wind speed (i.e Reynolds number).
3-The pattern of velocity distribution vector are independent of wind speed except that the magnitude of velocity vector increases when wind speed increased but the distribution pattern dependent of angles of pitch angles.
4-The pressure distribution is related to wind speed and angles of attack.
5-The pressure difference between the forward and leeward of the trough are depend on the pitch angle and the maximum difference occurs at ($\theta=90^{\circ}$).
6-Many recirculation regions are formed in the leeward of the trough and this formation depend on angle of attack.
7-The presence of stiffener make the trough more bluff body and the formation of vortex increased.
8-The presence of stiffener may be useful for enhancement of vortex induced vibration which is useful for dust removal techniques.

REFERENCES

[1]. morphy,L.M. "wind loading on tracking and field mounted solar collectors", Solar energy research institute, Golden, Colorado, 80401, 1980.
[2]. peterka,J.A. Z. Tan, B. Bienkiwicz, J. E. Cermak, Fort Collins, "Wind Loads on Heliostats and Parabolic Dish Collectors", Solar energy research institute, 1988.
[3]. Gunasena,N. U. "An experimental study of mean wind forces on hemispherical solar collectors", M.Sc thesis, Texas tech university, 1989.

[4]. Hosoya and J.A. Peterka,N." wind tunnel tests of parabolic trough solar collector", National renewable energy laboratory, 2008.
[5]. Naeeni, N. M. Yaghoubi, "Analysis of wind flow around a parabolic collector" Renewable Energy 32 (2007) 1898–1916.
[6].Ansys fluent reference theory. Twelve edition, 2009.
[7].Saha AK, Biswas G, Muralidhar K. Numerical study of the turbulent unsteady wake behind a partially enclosed square cylinder using RAANS. Int J Comput Methods Appl Mech Eng 1999;178:323–41.

Appendix A: Load Coefficients [4]

Wind load effects are characterized in terms of non-dimensional coefficients. The definitions of the load coefficients are:

Horizontal Force, fx $cf_x = \frac{f_x}{qLW}$

Vertical Force, fz $cf_z = \frac{f_z}{qLW}$

Pitching Moment, my, $Cm_y = \frac{my}{qLW^2}$

Where *fx*, *fz*, and *my* are the aerodynamic loads. *L* is the span-wise length, and *W* is the aperture width of the collector figure (1). The quantity, *q*, is the mean reference dynamic pressure measured at the pivot height of the solar collector, Hc, as given by $q = \frac{1}{2}\rho U^2$ Here *U* is the mean wind speed at the pivot height, and ρ is the density of air. Similarly, the pressure coefficient is expressed by

$$\mathrm{cp} = \frac{\mathrm{p}}{\mathrm{q}}$$

where *p* is the local pressure relative to the undisturbed ambient static pressure.

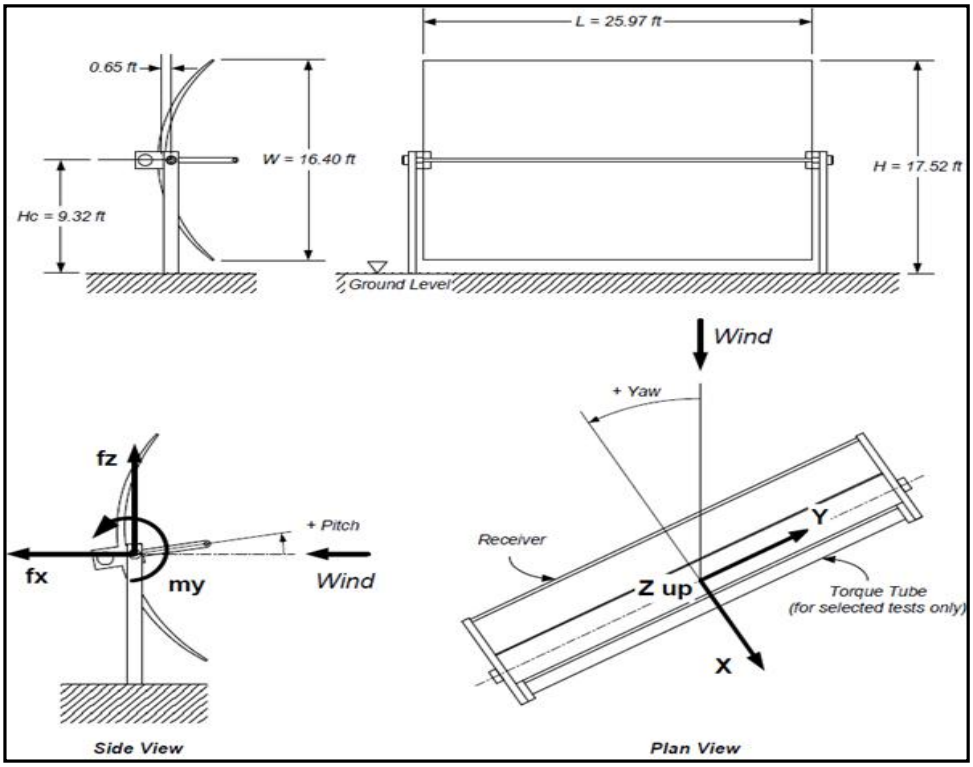

Figure (1) dimensions of parabolic trough used in experimental tests and description of attack angles [4]

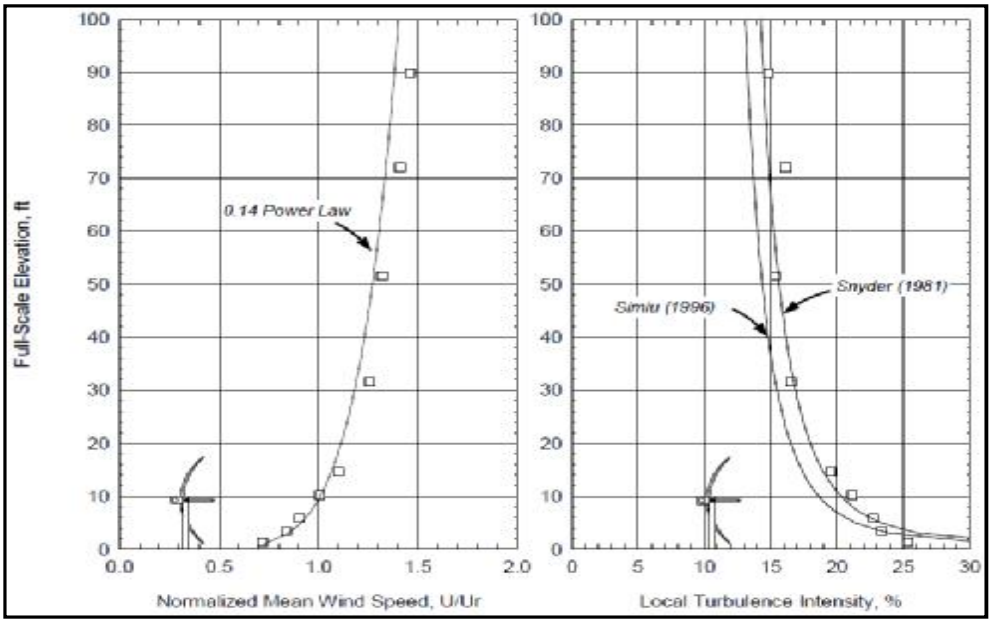

Figure (2) mean wind velocity profile and turbulent intensity simulated in experimental test [4].

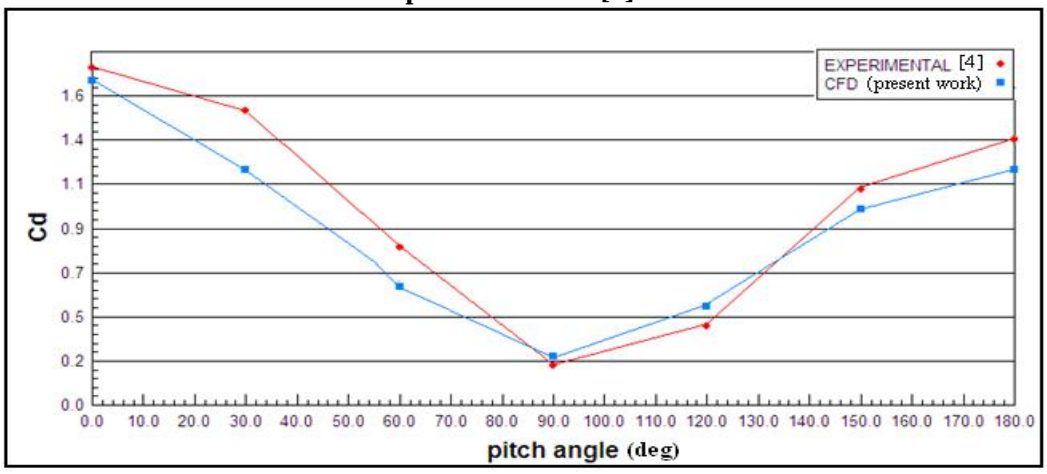

Figure (3) comparison between experimental and numerical results of drag coefficient for parabolic trough.

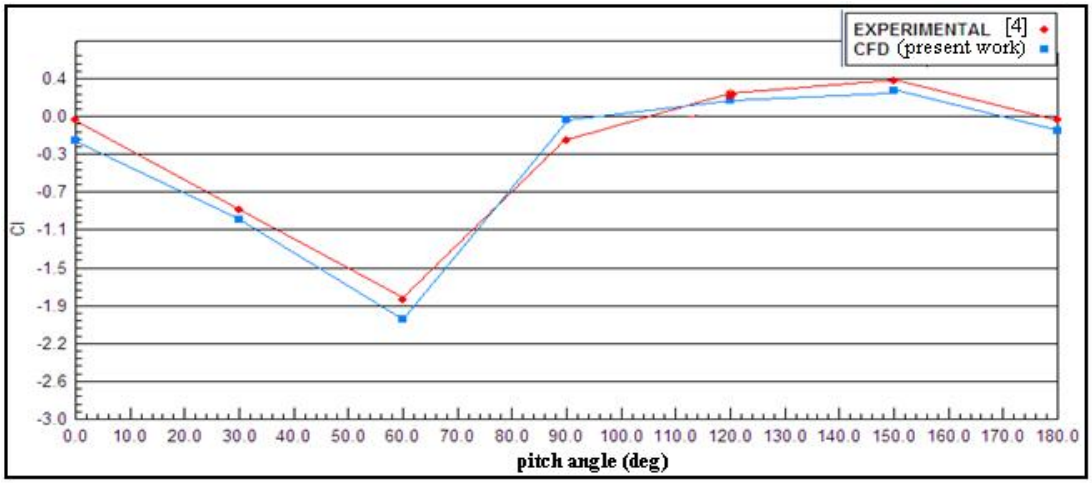

Figure (4) Comparison between experimental and numerical results of lift coefficient for parabolic trough.

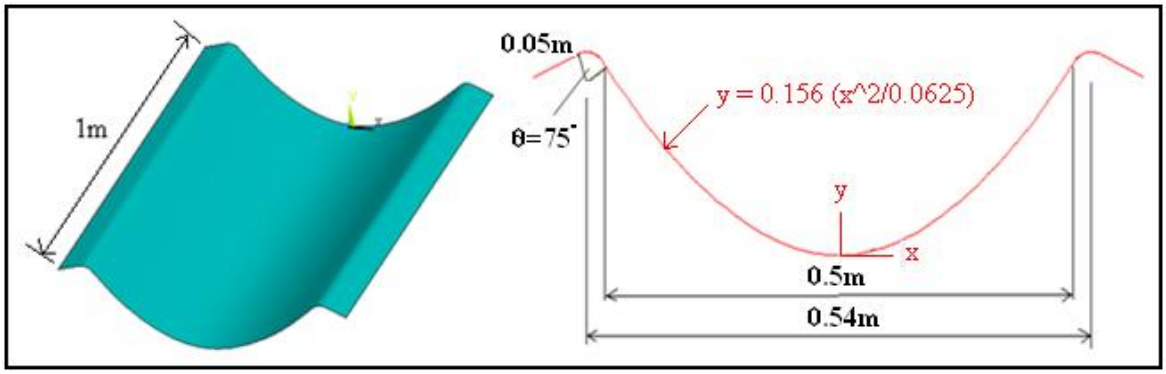

Figure (5) the dimensions and profile of the parabolic trough used in numerical simulation.

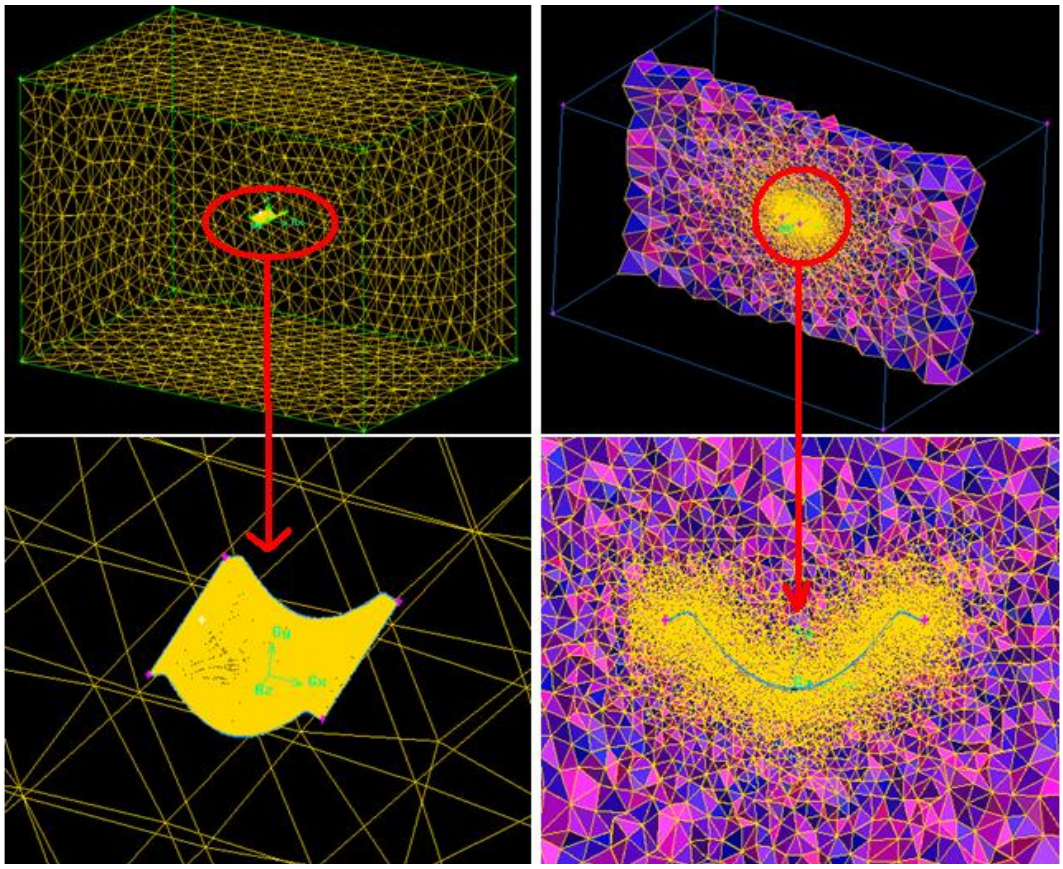

Figure (6) the domain and the mesh density distribution through the domain.

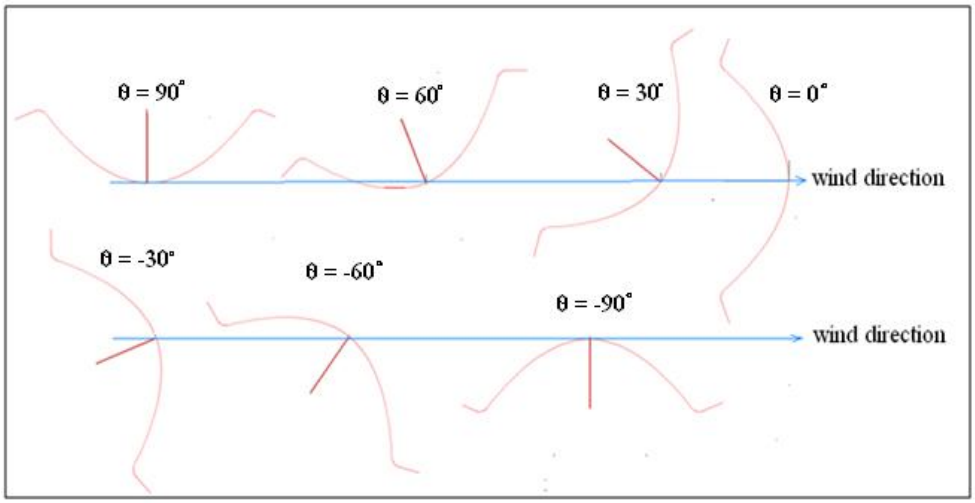

Figure (7) angles of attack (pitch angles) between the trough and wind flow.

Table (1) size of domain and mesh density corresponding to each pitch angle.

Pitch angle (deg)	Size of domain (L*W*H) (m^3)	Mesh density
0	20*12*8	2487385
30	20*12*10	2676275
60	20*12*12	2865392
90	20*12*15	3198476
120	20*12*12	2865392
150	20*12*10	2676275
180	20*12*8	2487385

Table(2) numerical results sensitivity to mesh density.

No.	Mesh density	Cd	Cl
1	1645298	0.6165	-2.2384
2	1818476	0.6383	-2.2845
3	1987463	0.6647	-2.4782
4	2178564	0.6844	-2.5103
5	2456837	0.7027	-2.5280
6	2678493	0.7134	-2.5282
7	2865392	0.7136	-2.5283

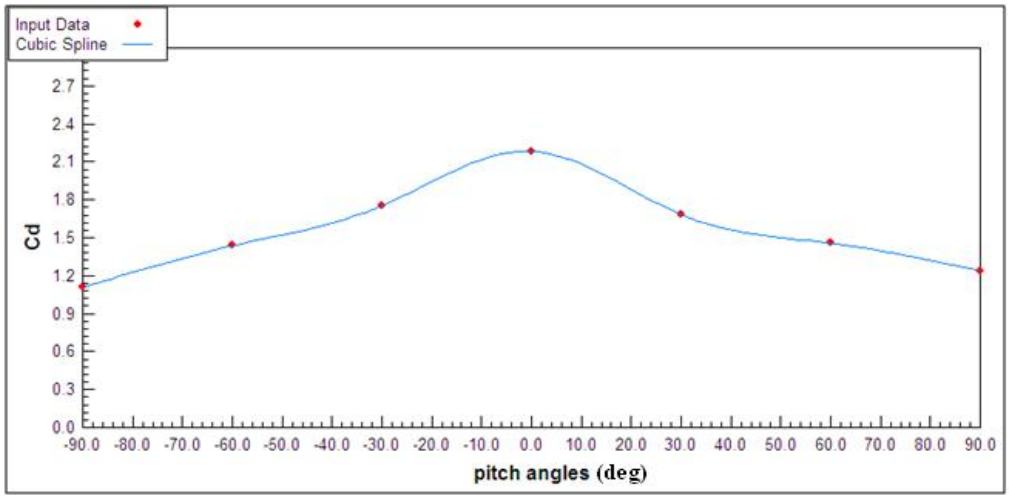

Figure (8) drag coefficient of parabolic trough obtained from numerical simulation.

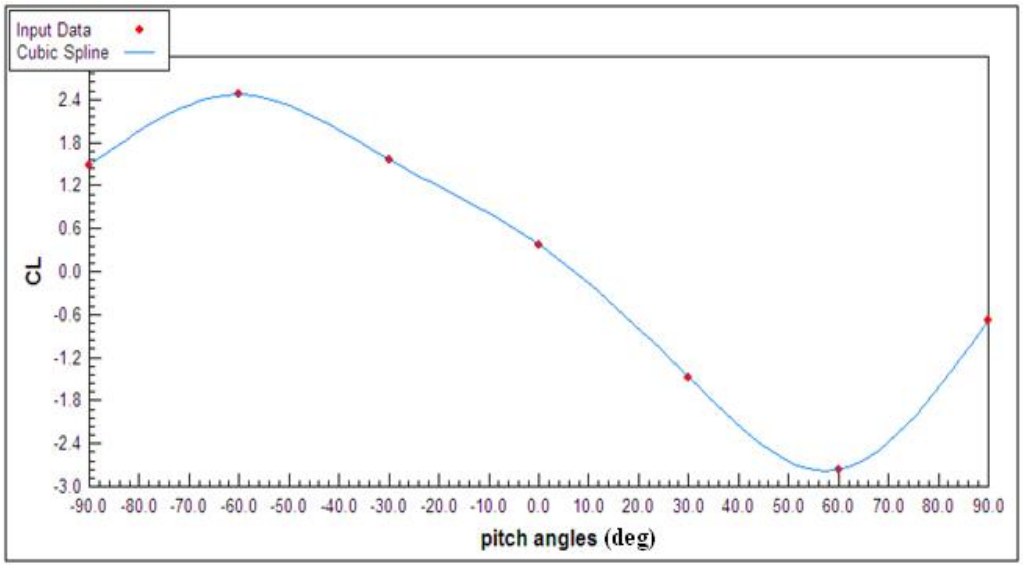

Figure (9) lift coefficient of parabolic trough obtained from numerical simulation.

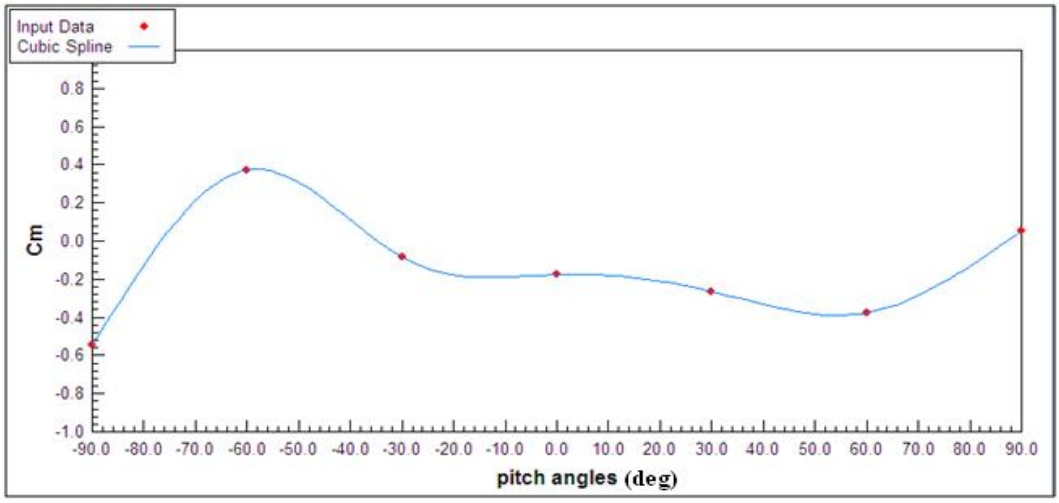

Figure (10) moment coefficient of parabolic trough obtained from numerical simulation.

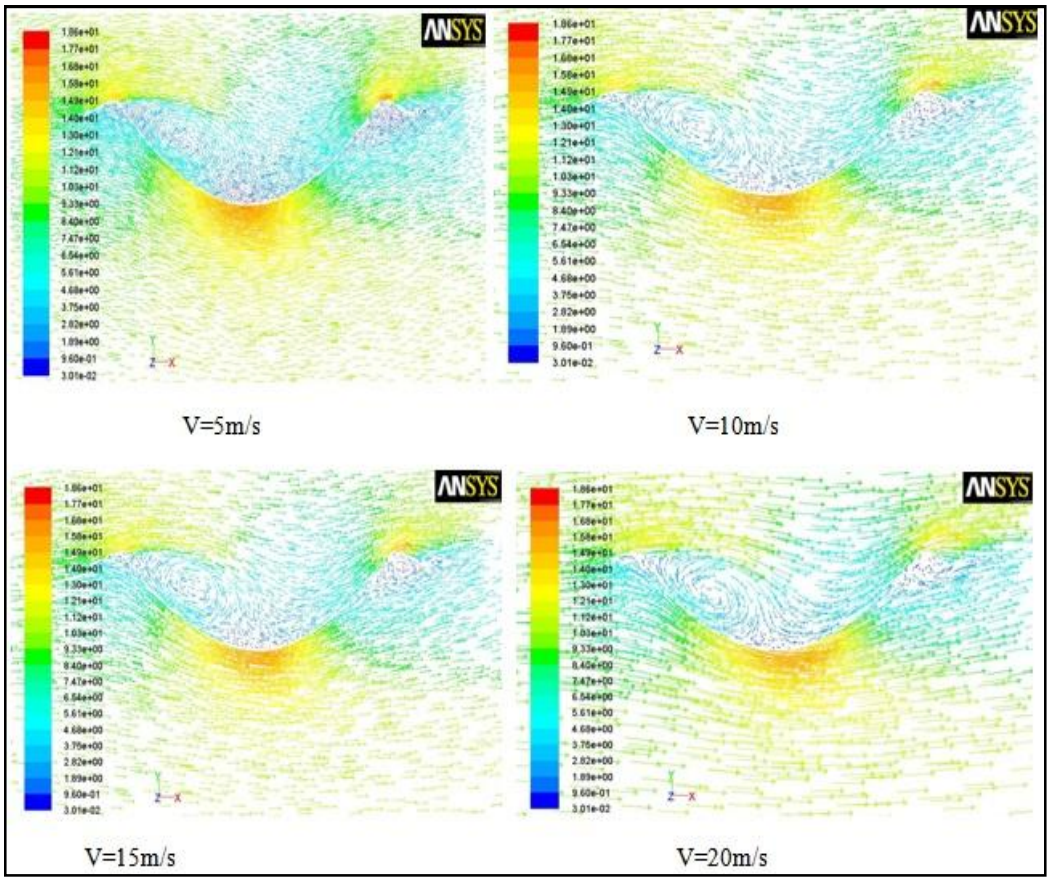

Figure (11) the velocity distribution vector around the trough for different velocities at pitch angles (θ=0).

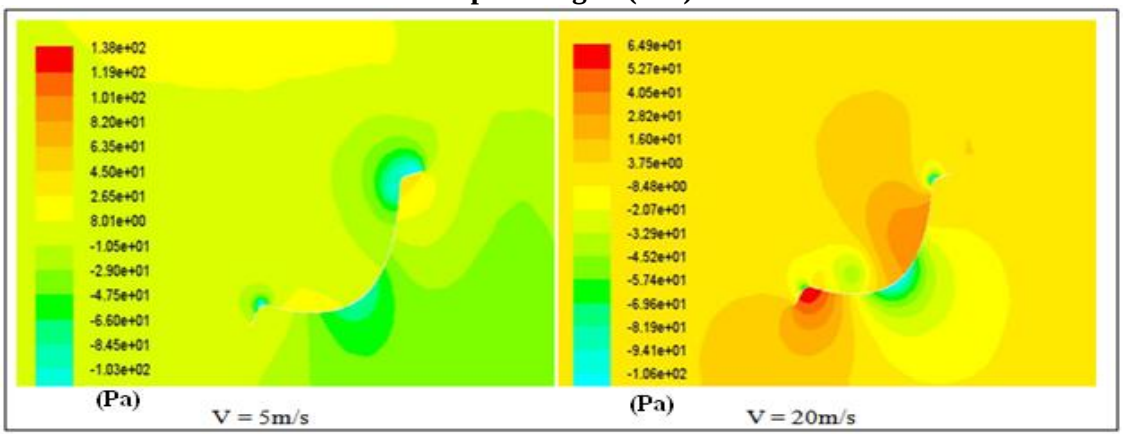

Figure (12) pressure distribution around the trough at pitch angle (θ = +60) for two velocities.

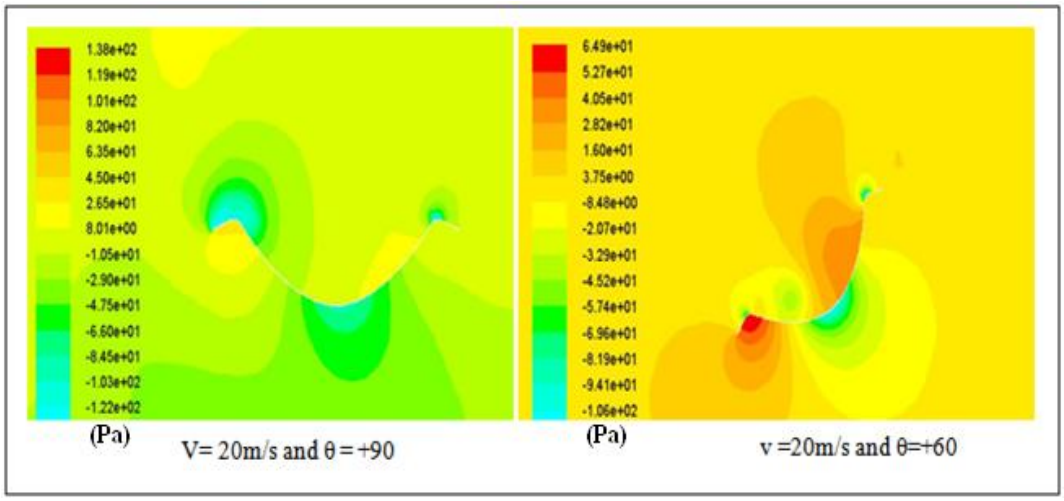

Figure (13) pressure distribution around the trough for two pitch angles at velocity 20 m/s

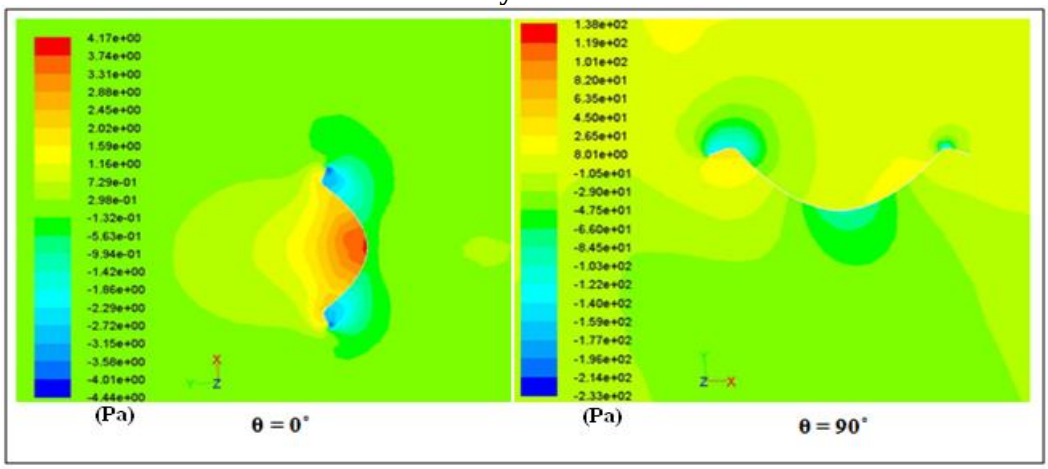

Figure (14) pressure diffrence between forward and leeward zones for two pitch angles at wind velocity20m/s.

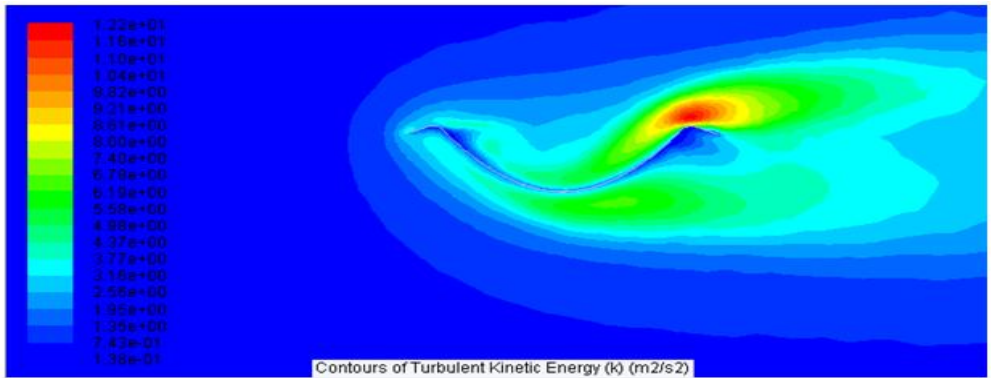

Figure (15) Contour of Turbulent Kinetic energy (k) m^2/s^2 at (θ = + 90°) and wind velocity 10 m/s.

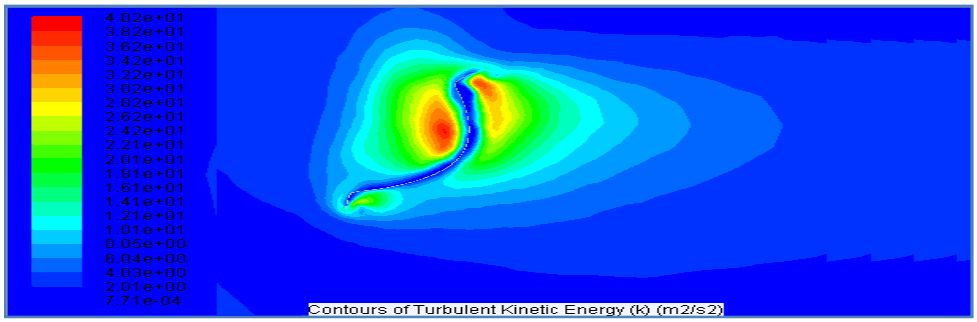

Figure (16) Contour of Turbulent Kinetic energy (k) m^2/s^2 at (θ = + 30°) and wind velocity 10 m/s.

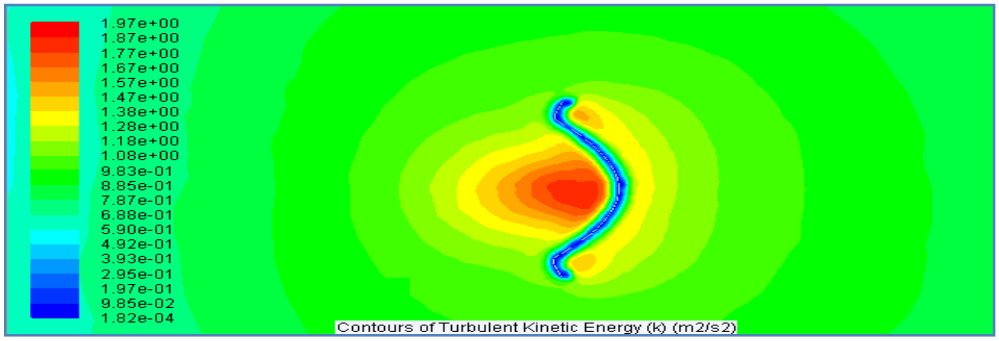

Figure (17) Contour of Turbulent Kinetic energy (k) m^2/s^2 at (θ = 0°) and wind velocity 10 m/s.